JACS
JOURNAL OF THE AMERICAN CHEMICAL SOCIETY
Article
pubs.acs.org/JACS

Partial Oxidation of Ethane to Oxygenates Using Fe- and Cu-Containing ZSM-5

Michael M. Forde,[†] Robert D. Armstrong,[†] Ceri Hammond,[†] Qian He,[‡] Robert L. Jenkins,[†] Simon A. Kondrat,[†] Nikolaos Dimitratos,[†] Jose Antonio Lopez-Sanchez,[†] Stuart H. Taylor,[†] David Willock,[†] Christopher J. Kiely,[‡] and Graham John Hutchings*[,†]

[†]Cardiff Catalysis Institute, School of Chemistry, Cardiff University, Main Building Park Place, Cardiff CF103AT, United Kingdom.
[‡]Department of Materials Science and Engineering, Lehigh University, 5 East Packer Avenue, Bethlehem, Pennsylvania 18015-3195, United States

Supporting Information

ABSTRACT: Iron and copper containing ZSM-5 catalysts are effective for the partial oxidation of ethane with hydrogen peroxide giving combined oxygenate selectivities and productivities of up to 95.2% and 65 mol kg_{cat}^{-1} h^{-1}, respectively. High conversion of ethane (ca. 56%) to acetic acid (ca. 70% selectivity) can be observed. Detailed studies of this catalytic system reveal a complex reaction network in which the oxidation of ethane gives a range of C_2 oxygenates, with sequential C−C bond cleavage generating C_1 products. We demonstrate that ethene is also formed and can be subsequently oxidized. Ethanol can be directly produced from ethane, and does not originate from the decomposition of its corresponding alkylperoxy species, ethyl hydroperoxide. In contrast to our previously proposed mechanism for methane oxidation over similar zeolite catalysts, the mechanism of ethane oxidation involves carbon-based radicals, which lead to the high conversions we observe.

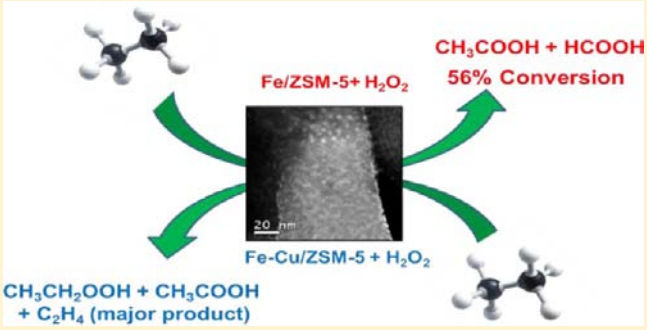

1. INTRODUCTION

Juxtaposed against the high global reserves of natural gas, primarily composed of methane and ethane, is the difficulty presented by the partial oxidation of such abundant lower alkanes under mild conditions. This has resulted in all commercially operated technologies for the activation of lower alkanes requiring highly energy intensive or non-environmentally benign processes. For example, the steam reforming of methane is operated on a large scale to produce synthesis gas for methanol synthesis or Fischer−Tropsch synthesis.[1] Ethanol, a commodity chemical with fuel applications, can be produced from ethene by acid catalyzed hydroxylation reactions.[2] However, ethene itself is produced by steam cracking of ethane or mixed hydrocarbon feedstocks, and the energy consumption of these processes accounts for a major portion of all energy used in petrochemical processes accompanied by high CO_2 emissions.[3] Although a process for the direct conversion of ethane to acetic acid using molybdenum mixed oxide catalysts has been described,[4,5] acetic acid is more normally manufactured on the industrial scale by methanol carbonylation (i.e., the BP Cativa Process).[6] A highly selective direct process of converting ethane to useful oxygenates (such as ethanol, acetic acid, or acetylaldehyde) could circumvent the need to use the indirect energy intensive and environmentally nonbenign processes that are currently employed.

Although there has been significant interest in lower alkane oxidation, there are few reports of selective ethane oxidation using heterogeneous catalysts at low temperatures. Shul'pin and co-workers[7] have reported that the titanium silicate (TS-1) was active for ethane oxidation using tertiary butyl hydroperoxide as oxidant but with low productivity. Lin and Sen[8] have also reported that palladium and platinum supported on carbon were active for the formation of acetic acid from ethane using an in situ hydroperoxy capture approach, in which the oxidant was prepared from hydrogen (derived from the water gas shift reaction) and oxygen during reaction. Vanadium-containing heteropolyacids have also been used to prepare the carboxylic acids from corresponding lower alkanes in $K_2S_2O_8$/CF_3COOH.[9] Aqueous $RhCl_3$ promoted by a Pd/C catalyst has also been tested for the conversion of methane into acetic acid.[10] Nevertheless, each of these approaches, in common with many similar homogeneously catalyzed systems,[11−15] requires a strong acid medium for significant activity and/or selectivity to be observed. Other approaches to direct oxidation of alkane generally require high temperature and pressure and operate at

Received: April 7, 2013
Published: June 26, 2013

   dx.doi.org/10.1021/ja403060n | J. Am. Chem. Soc. 2013, 135, 11087−11099

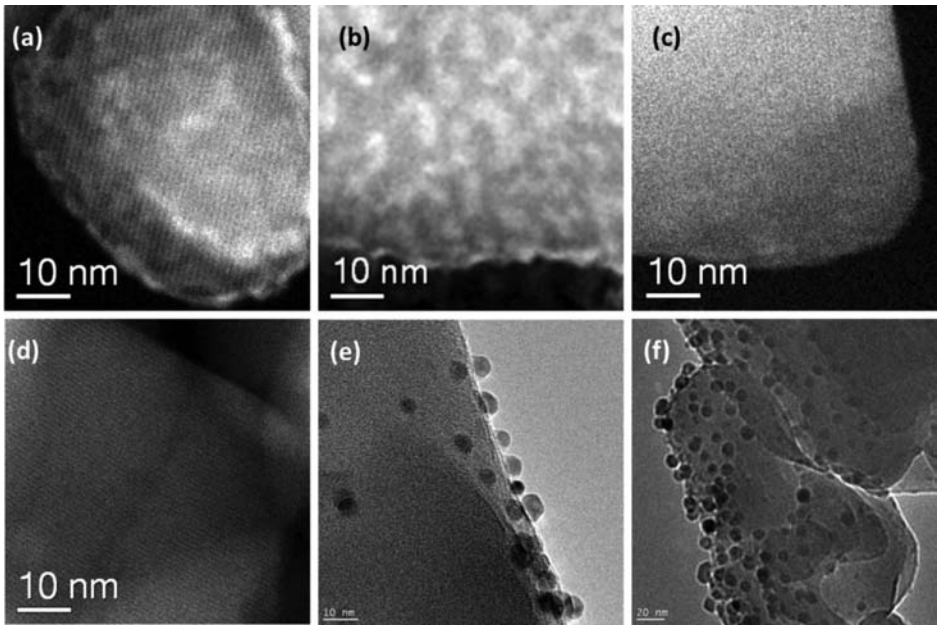

Figure 1. Electron micrographs of catalysts used in for ethane oxidation in this work. Representative STEM-HAADF images of (a) 0.4 wt % Fe/ZSM-5(30)$_{CVI}$ and (b) 2.5 wt % Fe/ZSM-5(30)$_{CVI}$ materials showing interconnected nanometer scale patches of Fe containing species(probably(FeOOH)) on the ZSM-5 surface in both catalysts which appear brighter in the HAADF images. Panels (c) and (d) show "plain" ZSM-5(30) support areas in these catalysts for comparison. Panels (e) and (f) show surface Cu species in 2.5 wt % Cu/ZSM-5(30). All materials were prepared by the CVI route and calcined in air.

low conversion, though high selectivity to partial oxygenated products can be attained. Notably, molecular oxygen has been used as the oxidant for lower alkane oxidation with silica supported metal oxides, particularly Ba_2O_3 and MgO, as catalyst by Otsuka and Hatano[16] which was a significant advance over the use of N_2O as the oxidant in these types of systems. Biocatalytic approaches utilizing methane monooxygenase enzymes for the transformation of ethane to ethanol have also been explored,[17] but with limited success. More recently, cytochrome P450 enzymes have been synthetically modified in order to obtain high catalytic rates to the alcohol product using ethane as a substrate,[18,19] but these systems have not yet been implemented on a larger scale.

We have recently shown that iron and copper modified zeolite ZSM-5 catalysts are highly efficient in oxidizing methane to methanol, using hydrogen peroxide as an oxidant,[20−22] and in this paper we now extend the work to ethane oxidation. We show that iron and copper modified ZSM-5 has high catalytic activity for the partial oxidation of ethane to oxygenates (i.e., ethyl hydroperoxide, ethanol, acetylaldehyde, acetic acid, glycolic acid, methyl hydroperoxide, methanol, formic acid) and ethene, under mild aqueous phase conditions using hydrogen peroxide as the oxidant. These reuseable catalysts achieve up to 56% conversion at an oxygenate selectivity of over 95% (ca. 70% to acetic acid) at 50 °C without the use of acid promoters. The production of ethene from ethane in a low temperature aqueous phase reaction is also reported for the first time.

2. RESULTS AND DISCUSSION

2.1. Catalyst Synthesis and Preliminary Characterization. In the catalytic studies that follow we have utilized two materials from our previous studies[20−22] on the oxidation of methane with H_2O_2 as oxidant, namely, H-ZSM-5(30) (Zeolyst) and 0.5 wt % Fe-Silicalite-1 prepared by hydrothermal synthesis in-house. Both materials were used after heat treatment (550 °C in air, 750 °C steaming, respectively) and were extensively characterized in our previous reports.[20−22] In H-ZSM-5(30), we have reported that the trace impurities of iron exist as cationic iron species at the ion exchange sites and postulated that these are dimeric μ-oxo-hydroxo iron species,[20,21] which is in keeping with previous efforts to identify the active iron species in ZSM-5 materials.[23−25] For 0.5 wt % Fe-Silicalite-1, we also found that the iron, after extensive steam treatments, migrated from substituted framework positions to form extra-framework iron species within the zeolite micropores and then small iron clusters and external iron oxides upon harsher heat treatment conditions.[22]

Since the addition of Fe to ZSM-5(30) has been shown to markedly increase the catalyst productivity in methane oxidation,[20] we also prepared Fe/ZSM-5(30) by a post synthesis deposition technique, the chemical vapor impregnation (CVI) method. In this preparation method, iron(III) acetylacetonate was physically mixed with H-ZSM-5(30) and heated under constant vacuum to achieve vaporization and deposition of the organometallic precursor onto the support in one step (see the Supporting Information (SI) for full experimental details). The adsorbed metal precursor was then decomposed by subsequent heat treatments. The technique has the advantage of bypassing the use of (i) solvents (as in the case of incipient wetness, sol-immobilization, and deposition precipitation methods) and (ii) the iron(III) chloride precursors used in traditional sublimation techniques with ZSM-5(30), and allows facile preparation of catalyst materials in a simple, reproducible, and scalable manner. Typically, the CVI method generates very highly dispersed supported nanoparticles (usually ∼1−3 nm in size on amorphous supports as in the case of Fe/SiO_2 shown in Figure S1 (SI)). As shown by our HR-TEM studies, Fe/ZSM-5(30) catalysts prepared in this way comprise iron-containing species that form a porous

dx.doi.org/10.1021/ja403060n | J. Am. Chem. Soc. 2013, 135, 11087−11099

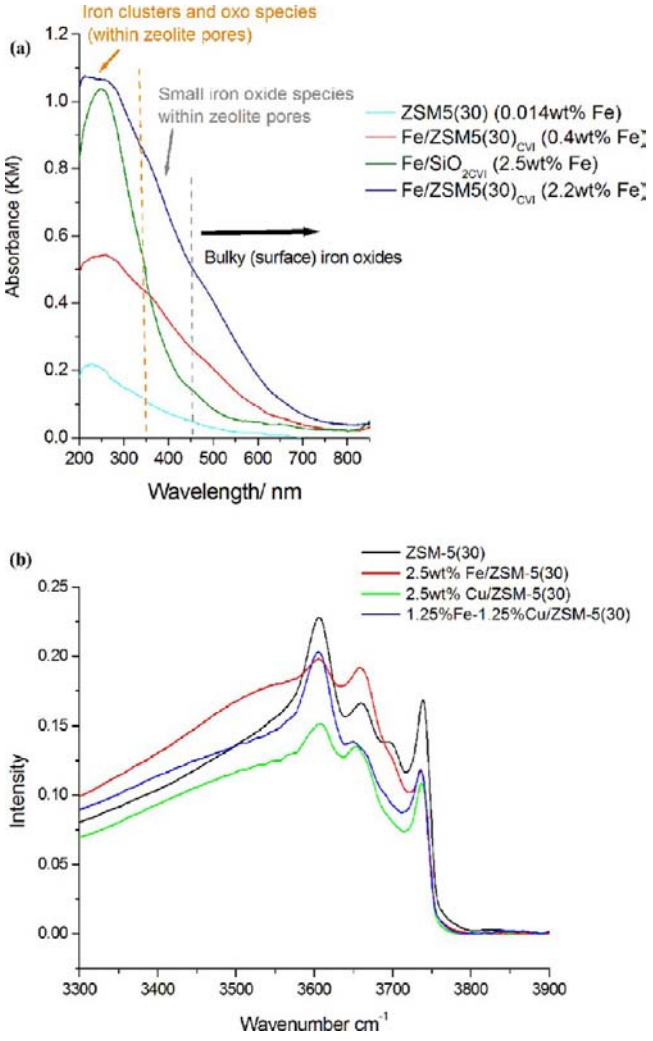

Figure 2. (a) UV−vis spectra of iron catalysts prepared by CVI and used in the oxidation of ethane with H_2O_2 as oxidant. The three main regions of iron species in ZSM-5(30) (200−350, 350−400, and >450 nm) are shown on the spectra. The spectrum of 2.5 wt %Fe/SiO_2 prepared by CVI is also shown for comparison. (b) IR spectra in the OH vibrational region for catalysts used in this work. All catalysts were calcined at 550 °C in air and spectra recorded at room temperature.

film on the zeolite surface (Figure 1a−d). We postulated that iron species may also be found within the zeolite crystals, as opposed to the external surface, and performed preliminary studies using UV−vis and IR spectroscopy. It is well accepted that iron species in ZSM-5 give rise to UV−vis bands between (i) 200−250 nm (isolated Fe^{3+} in framework positions), (ii) 250−350 nm (isolated or oligonuclear extra-framework Fe species), (iii) 350−450 nm (iron oxide clusters), and (iv) above 450 nm (larger iron oxide aggregates on the external crystal surface).[26−29] For the Fe/ZSM-5(30) catalysts prepared by CVI, our UV−vis analysis (Figure 2a) shows that the iron species are distributed among all four speciation groups outlined above, but it is apparent that a significant amount of iron is found as isolated iron clusters, oligomeric species, and cationic species at exchange sites within the zeolite pores. The presence of iron species on the external zeolite surface is corroborated by the HRTEM studies, and thus, it is clear that there is also a significant amount of iron as iron/iron oxide clusters within the zeolite pores or as cationic extra-framework species. Without accurate absorption coefficients, it is not possible to quantify the speciation distribution but more information could be attained by IR spectroscopy of the materials, particularly the OH vibrational region (see Table S2 (SI) for assignments).[30−36]

Comparison of the IR spectra for ZSM-5(30) and 2.5 wt % Fe-ZSM-5(30) shows that the peak attributed to OH groups coordinated to tetrahedrally coordinated framework Al^{3+} (3607 cm^{-1})[33,34] decreases on incorporation of Fe into the catalyst with a corresponding increase in the peak attributed to OH groups coordinated to extra-framework T-atoms (3660 cm^{-1}).[31,32,35] Additionally, there is increased intensity of the peak at 3520 cm^{-1} (bridging OH groups with extra electrostatic character).[36] These changes are accompanied by the near disappearance of the band attributed to OH groups in defect sites (hydroxyl nests) at 3700 cm^{-1}[36]and some loss of terminal silanols/nonacidic silanols on the ZSM-5 outer surface (peak at 3737 cm^{-1})[30,36] upon incorporation of Fe into the catalyst. These data strongly support the increased extent of migration of framework Al^{3+} (dealumination) and subsequent formation of extra-framework T-atom species (Fe^{3+} or Al^{3+} based) as well as the additional modification of the Bronsted acid character upon incorporation of Fe into the catalyst.

This is also the case for the incorporation of Cu^{2+} into the ZSM-5(30) where even greater loss of framework Al^{3+} along with a broader band at 3520 cm^{-1} is observed. An additional shoulder peak on the band at 3650 cm^{-1} is also observed in the spectrum of Cu/ZSM-5(30). These modifications result from the incorporation of Cu into ZSM-5(30) and support the hypothesis that the Cu ions are also located in the zeolite pores (as cationic exchange species or as clusters copper species/oxide). HR-TEM studies (Figure 1e,f) also demonstrate that copper oxide species are present on the external zeolite surface. In the case of the bimetallic Fe−Cu/ZSM-5(30) catalyst, the OH vibrational region is very much akin to the ZSM-5(30) material with the exception of a shift in the wavenumber of the peak attributed to OH groups coordinated to extra-framework T-atoms[31,32,35,36] (3662 to 3650 cm^{-1}) and a clearly visible shoulder peak at 3668 cm^{-1}, which is also observed with Cu/ZSM-5(30). This suggests that the simultaneous effect of incorporation of Fe and Cu affects the internal structure of the ZSM-5 differently to the monometallic catalysts. Further detailed studies of the materials by in situ techniques are underway, and another publication will be focused on the nature of the metal species in these catalysts.

2.2. Comparison of the Activity of Fe and Cu Containing ZSM-5(30) Catalysts for Ethane Oxidation. For our initial studies, we used H-ZSM-5(30) (Zeolyst, SiO_2:Al_2O_3 = 30) as this material showed the highest intrinsic activity among the zeolites we investigated for methane oxidation with hydrogen peroxide in water.[20,21] Having previously identified that trace impurities of iron (140 ppm) in ZSM-5(30) were responsible for the selective oxidation of methane, we considered that ethane oxidation may proceed with an even higher catalytic productivity due to the greater availability of substrate, since ethane is more soluble than methane in water (56 versus 22.7 mg_{gas}/L_{water} at 20 °C)[37] and has a lower C−H bond strength than methane (423.29 versus 439.57 kJ mol^{-1}).[38] Under similar experimental conditions to those reported previously,[20] we observed that H-ZSM-5(30) achieved a similar level of conversion with ethane when compared to methane (Table 1, entries 1, 2), suggesting that the conversion was independent of the initial concentration of ethane substrate under these specific reaction conditions. Fe/

dx.doi.org/10.1021/ja403060n | J. Am. Chem. Soc. 2013, 135, 11087−11099

Table 1. Aqueous Phase Ethane Oxidation Using Various Fe and Cu Modified ZSM-5(30) Catalysts[a]

				selectivity to aqueous phase products %[c]						selectivity to gas phase products %[d,e]			
entry	catalyst	alkane	conversion %[b]	MeOOH	MeOH	HCOOH	EtOH	CH_3COOH	others[h]	C_2H_4	CO_x	TOF[f]	H_2O_2 used/ products[g]
1	ZSM-5(30)	CH_4	0.2	23.3	19.5	54.7					2.5	1211.4	24.4
2	ZSM-5(30)	C_2H_6	0.2	2.4	5.7	16.7	26.2	36.6	0.0	7.6	1.9	1211.4	28.1
3	1.1%Fe/ZSM-5(30)	C_2H_6	3.3	0.4	3.8	15.7	22.6	54.6	0.0	0.4	2.5	137.2	5.0
4	2.5%Fe/ZSM-5(30)	C_2H_6	2.2	0.3	3.8	14.9	24.3	53.7	0.3	0.6	2.3	77.8	5.5
5	2.5%Fe/SiO_2	CH_4	0.1	37.8	11.5	5.7			31.5		13.5	4.3	133.3
6	2.5%Fe/SiO_2	C_2H_6	0.3	0	1.2	1.7	8.5	13.1	67.1	3.5	4.9	12.9	45.0
7	0.5%Fe/Sil-1[i]	C_2H_6	0.4	1.3	3.2	6.8	40.0	30.4	14.4	1.5	2.4	66.5	20.7
8	0.4%Fe/ZSM-5(30)	C_2H_6	1.1	1.0	5.0	13.8	18.9	49.2	6.0	4.7	2.4	233.2	7.8
9	2.4%Fe/ZSM-5(30)[j]	C_2H_6	0.6	4.2	2.1	11.5	12.0	50.5	14.9	3.4	1.4	20.4	10.6
10	2.5%Cu/ZSM-5(30)	C_2H_6	0.2	0.0	5.4	0.0	33.6	18.2	10.0	30.2	2.6	7.7	18.3
11	1.25%Cu-1.25%Fe/ ZSM-5(30)	C_2H_6	1.6	0.1	7.3	0	25.9	30.9	0.0	34.2	1.6	32.6	6.1
12	2.5%Cu-2.5%Fe/ZSM-5(30)	C_2H_6	1.4	0.0	11.4	0	24.3	24.1	1.1	38.2	0.9	28.5	9.2
13	1.1%Fe/ZSM-5(30)	C_2H_4	52.0	0.0	0.0	49.1	0.0	0.6	0.0		50	21.1	n.d
14	2.5%Cu/ZSM-5(30)	C_2H_4	14.6	56.6	7.8	0.0	0.0	16.6	0.0		19.0	2.8	n.d
15	1.25%Cu-1.25%Fe/ ZSM-5(30)	C_2H_4	28.4	2.4	0.0	0.0	0.0	5.6	0.0		92	2.8	n.d.
16	2.5%Fe/ZSM-5(30)	C_2H_6	56.4	1.1	2.6	21.1	4.7	69.3	0	0.2	1.1	150.7	5.6
17	1.25%Cu-1.25%Fe/ ZSM-5(30)	C_2H_6	33.8	0.5	8.7	6.2	8.5	49.9	12.6	12.8	0.7	52.0	13.4

[a]Reaction conditions for entries 1-12: 28 mg of catalyst, 10 mL reaction volume, $[H_2O_2]$ 0.5 M, reaction time 0.5 h, $P(C_2H_6)$ = 20 bar, T_{rxn} = 50 °C, stirring rate 1500 rpm. All catalysts were prepared by CVI and calcined at 550 °C in static air except where noted. Reaction conditions for entries 13-15: 28 mg of catalyst, 10 mL reaction volume, $[H_2O_2]$ 0.5 M, reaction time 0.5 h, 10 bar 1%C_2H_4/N_2, T_{rxn} = 50 °C, stirring rate 1500 rpm. Reaction conditions for entries 16, 17: 54 mg of catalyst, 20 mL reaction volume, $[H_2O_2]$ 1.0 M, reaction time 0.5 h, $P(C_2H_6)$ = 5 bar, T_{rxn} = 50 °C, stirring rate 1500 rpm. [b]Based on moles C in product/initial moles C in substrate. [c]Based on C using product amounts detected by ^{1}H NMR. [d]Based on C using products detected by GC-FID. [e]Methane has not been not included but can be quantified by GC-FID only after tedious methods to remove all traces on methane from the reactor gas lines and the GC column. For all entries, methane is observed in trace amounts (<1 μmol) in the gas phase. [f]Defined as mol(product)$^{-1}$ mol (metal)$^{-1}$ h^{-1} and is based on the experimentally determined metal loading. [g]Unreacted H_2O_2 determined by titration against Ce^{4+} (acidified) using Ferroin as indicator. [h]CH_2O for methane as the substrate and CH_3CH_2OOH (minor) + CH_3CHO (main) for ethane as the substrate. [i]Prepared by hydrothermal synthesis followed by calcination at 550 °C in flowing air for 3 h. [j]Prepared by ion exchange from $Fe(NO_3)_3$ followed by calcination at 550 °C in static air for 3 h; Me = CH_3 and Et = C_2H_5.

ZSM-5(30) of 1.1 wt % prepared by CVI[39] gave a higher conversion than 2.5 wt % Fe/ZSM-5(30) (3.3% versus 2.2% conversion after 0.5 h reaction) with an oxygenate selectivity of over 95%, which represents a total productivity of 47 mol product kg(cat)$^{-1}$ h^{-1} or a turnover number (TON) of ca. 123 mol (product) mol (Fe)$^{-1}$ for the 1.1 wt % Fe catalyst (Table 1, entries 3 and 4).[40] The major product obtained is acetic acid (>50%), together with ethanol and formic acid, as well as minor amounts of methanol, methyl hydroperoxide and ethene.

Dimeric iron-μ-oxo or oligiomeric iron species have been proposed as the active site of ZSM-5(30) in a number of studies,[23−25] but we note that in our materials iron clusters and iron oxide particles may be present within the ZSM-5 channels and also on the external zeolite surface. To investigate the possible contribution of various iron species, we utilized three different materials, namely, 2.5 wt % Fe/SiO_2 prepared by CVI, 0.5 wt % Fe-Silicalite-1 prepared by hydrothermal synthesis and steamed, and 0.4 wt % Fe/ZSM-5(30) prepared by CVI. Fe/SiO_2 of 2.5 wt % could be used to assess the activity of small surface iron oxide nanoparticles (<3 nm), since we have already reported that Fe/SiO_2 (prepared by incipient wetness) is also active for methane oxidation and is stable under reaction conditions[41] though much less active than H-ZSM-5(30) or 2.5 wt % Fe/ZSM-5(30).[20,21] Fe/SiO_2 of 2.5 wt % prepared by CVI had small surface iron oxides (<3 nm, Figure S1 (SI)), and we observed an increase in conversion when ethane replaced methane as the hydrocarbon reactant (Table 1, entries 5, 6) which is in keeping with the higher solubility and weaker C−H bond strength in ethane, rendering it to be intrinsically more reactive than methane. Moreover, though the Fe/SiO_2 showed a level of ethane conversion, comparable to that of H-ZSM-5, the product distribution differed markedly in that the major products were ethyl hydroperoxide and acetylaldehyde (ca. 67% of the total products, Table 1, entries 2, 6). These observations suggest that small surface iron oxide species can contribute to the products in the oxidation of ethane using hydrogen peroxide and notably in the absence of pronounced acidity (as compared to heat treated ZSM-5 based materials) there was low selectivity to C_1 products.

Our 0.5 wt %Fe-Silicalite-1 prepared by hydrothermal synthesis[20−22] and steamed prior to use had no external iron oxide species but the iron was previously found to be in isolated framework lattice positions and as cationic extra-framework species (isolated species and oligomeric species)[22] in the absence of Al^{3+}. The 0.4 wt %Fe/ZSM-5(30) catalyst prepared by CVI would have external iron oxide species as well as extra-framework iron species at cationic exchange sites and other iron clusters within the zeolite pores in the presence of Al^{3+}. In the oxidation of ethane we observed that the Fe-Silicaite-1 catalyst had ca. half the catalytic activity of 0.4 wt %Fe/ZSM-5(30)

dx.doi.org/10.1021/ja403060n | J. Am. Chem. Soc. 2013, 135, 11087−11099

Scheme 1. Oxidation of ^{13}C Labeled Ethanol and Acetic Acid over ZSM-5(30) Catalysts in the Aqueous Phase with H_2O_2 as Oxidant at 50°C

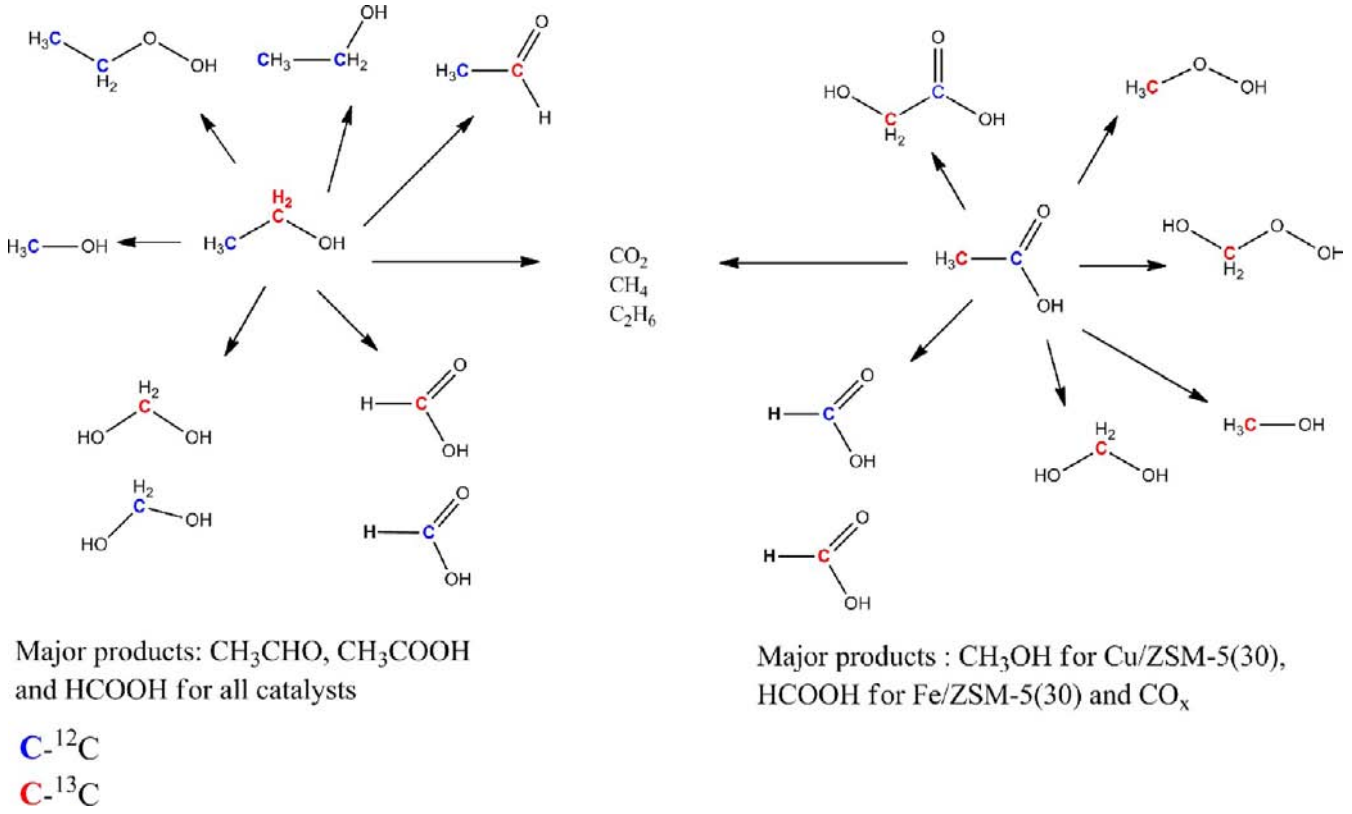

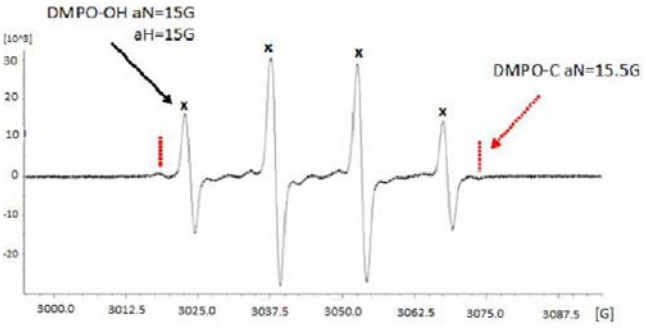

Figure 3. Electron paramagnetic resonance (EPR) spectrum of radicals trapped by 5,5′-dimethylpyrrolidine (DMPO) added to the reaction mixture at the start of the reaction for the oxidation of ethane (20 bar) using a calcined 2.5 wt %Fe/ZSM-5(30) catalyst (27 mg) and H_2O_2 (0.5 M in 10 mL water) for 5 min. The EPR spectrum was collected at room temperature after thawing out the reaction-radical trap mixture which was frozen immediately upon mixing. Carbon and hydroxyl radical adducts are clearly observed.

prepared by CVI with both materials having similar decomposition of H_2O_2 (Table 1, entries 7, 8; H_2O_2 used: products ratio of 20.7 versus 7.8 respectively). Since the iron content of both catalysts were nearly identical and they both have the MFI structure, it follows that the catalytic activity is not merely a function of the total iron content but that the speciation distribution of iron is pivotal. Also, since the CVI material had a significant amount of iron on the external zeolite surface this material could not have nearly as much iron available to form cationic species within the zeolite pores (i.e., extra-framework iron species, iron oligomers, and clusters) but still displayed higher catalytic activity. Therefore, we propose that multiple iron species may be involved in the oxidative pathways (to varying extents) and the CVI route allows the preparation of a very active catalyst due to the deposition of highly dispersed surface iron species on the acidic support or the formation of different iron species within the zeolite pores (as compared to previous work). This proposal is supported by the lower ethane oxidation activity of calcined 2.53% wt Fe/ZSM-5(30) prepared by traditional ion exchange and its higher usage of the oxidant (H_2O_2 used: products ratio of 10.6 for the ion exchange catalyst and 5.5 for the analogous CVI catalyst; Table 1, entries 4 and 9). We will further explore this phenomenon in relation to detailed characterization studies in a future paper.

We noted that the major product with H-ZSM-5(30) and Fe/ZSM-5(30) was acetic acid and postulated that ethanol selectivity may be increased by the addition of Cu to the catalyst since we have previously found that Cu was an effective additive to ZSM-5(30) for achieving high selectivity to methanol over formic acid in the methane oxidation reaction.[20] 2.5 wt % Cu/ZSM-5 (30) by CVI showed a comparable level of conversion of ethane as compared to ZSM-5(30) (Table 1, entry 10). However, as previously observed in our studies focusing on methane oxidation, a markedly different product distribution was observed in the presence of Cu. In this case, the selectivity to ethanol and ethene is significantly higher, and though acetic acid is still observed it is produced at a much lower selectivity than for ZSM-5(30) or Fe/ZSM-5(30) (18% versus 36−56% respectively). Based on our previous findings, the data suggests that the influence of Cu in arresting the overoxidation of the C_1 alcohol to formic acid in the methane oxidation reaction also occurs in the ethane system, as formic

dx.doi.org/10.1021/ja403060n | J. Am. Chem. Soc. 2013, 135, 11087−11099

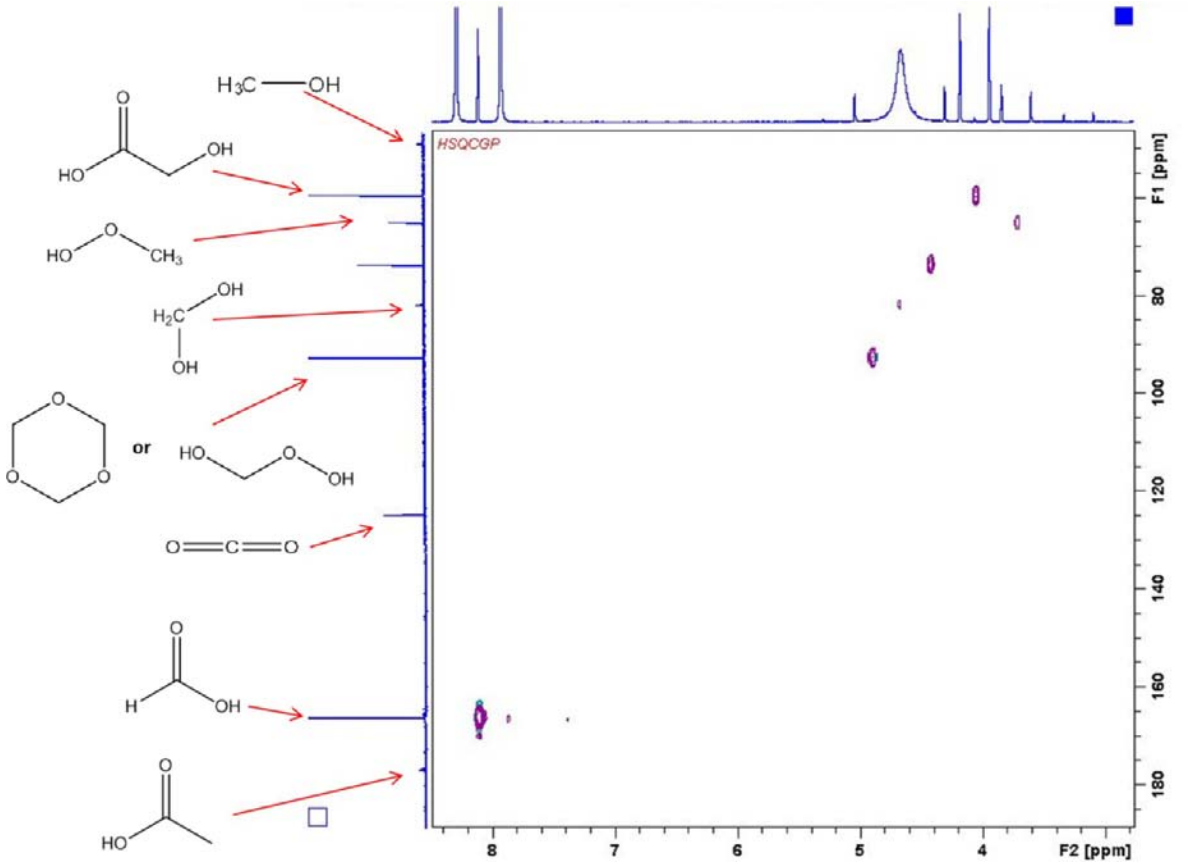

Figure 4. Expanded region of an HSQC-NMR spectrum of the oxidation of $^{13}CH_3C{=}O(OH)$ using Fe/ZSM-5(30) and H_2O_2 in D_2O. The assigned structures are shown on the left of the spectrum. Full details are given in Figures S5 (SI). ^1H NMR, top spectrum trace; ^{13}C NMR, left spectrum trace.

acid is not observed even though methanol is detected as a reaction product. However, the ability of Cu to eliminate the overoxidation of ethanol to acetic acid does not hold in the case of ethane oxidation.

An additional and somewhat unexpected benefit of the Cu-containing system is the significant selectivity to ethene observed. As demonstrated in Table 1, the use of 1.25 wt % Fe-1.25 wt %Cu/ZSM-5(30) or 2.5 wt %Fe-2.5 wt %Cu/ZSM-5(30) catalysts, prepared by simultaneous deposition of iron and copper onto ZSM-5(30) by CVI, gave high selectivity to ethene (34−38%) (Table 1, entry 11, 12) at a similar ethane conversion as observed with the monometallic Fe-containing analogues. These bimetallic catalysts also show higher selectivity to methanol and lower selectivity to acetic acid than the analogous Fe/ZSM-5(30) catalyst. We consider that the presence of C_1 oxygenates in the reaction products suggests the occurrence of either (i) C−C scission in C_2 products or (ii) oxidative pathways involving methyl radicals derived from the direct C- C scission of ethane. For the former process, one would expect formic acid to be observed in all cases regardless of the metal additive (Fe or Cu) since all catalysts were prepared from H-ZSM-5(30) which itself produces acetic acid and formic acid when employed as the catalyst (Table 1, entry 2 and Tables S3, S4). However, the absence of formic acid when using the Cu and Fe−Cu modified ZSM-5 catalysts suggests that either acetic acid has an enhanced stability in the presence of a Cu modified catalyst, or that other pathways to C_1 oxygenates (besides C−C cleavage of the C_2 reaction products) are in operation. Furthermore, the production of both ethene and methane from ethane suggests that carbon based radicals may be implicated in the reaction mechanism. These observations led us to perform in-depth mechanistic studies for ethane oxidation in order to establish the most probable reaction pathway.

2.3. Mechanistic Studies. *2.3.1. Oxidation of Ethanol and Acetic Acid by Fe and Cu/ZSM-5(30) Catalysts.* To estimate the possible level of absorption of the reaction products onto the catalyst we stirred the Fe and Cu modified ZSM-5 under N_2 at 50 °C in ethanol or acetic acid solutions (0.05 M). ^1H NMR analysis of these solutions after interaction with the catalysts showed that 10−20% of the substrates were absorbed in the absence of hydrogen peroxide (Figure S2 (SI)) and hence a carbon balance of 80−90% could be expected in our catalysis studies. We performed the oxidation of ethanol and acetic acid (starting concentration was 0.05 M, which is similar to the concentrations obtained during ethane oxidation) in the presence of hydrogen peroxide under N_2 at 50 °C. When using ethanol as a substrate we observed its oxidation to acetic acid along with the formation of methyl hydroperoxide, methanol or formic acid (refer to Figure S3 and Table S3 (SI)). The extent of oxidation is dependent on the presence of Fe or Cu, but the 2.5 wt % Cu/ZSM-5(30) catalyst does not produce formic acid under these test conditions, which is in agreement with our previous studies.[20] Moreover, acetic acid is converted to formic acid or methanol and CO_x by both catalysts at a lower rate than the oxidation of ethanol (Figures S3, S4 and Table S3 (SI)). The conversion of acetic acid to formic acid has been noted in earlier work by Lin and Sen using

dx.doi.org/10.1021/ja403060n | J. Am. Chem. Soc. 2013, 135, 11087−11099

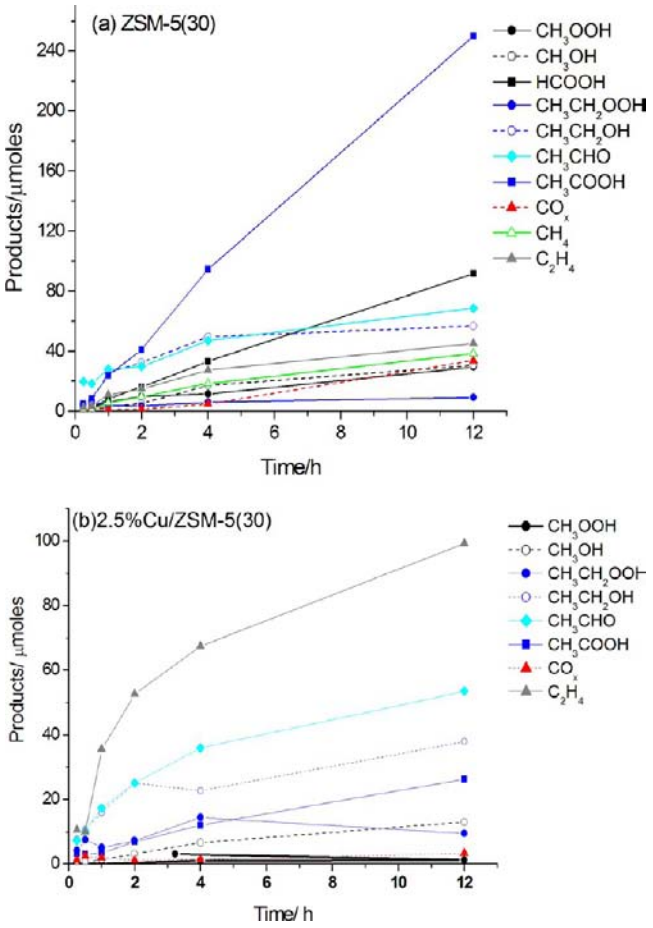

Figure 5. Time-online analysis for partial ethane oxidation using (a) ZSM-5(30) and (b) 2.5 wt % Cu/ZSM-5(30) catalysts in the aqueous phase with H_2O_2 (1 M in water) as oxidant at 50 °C.

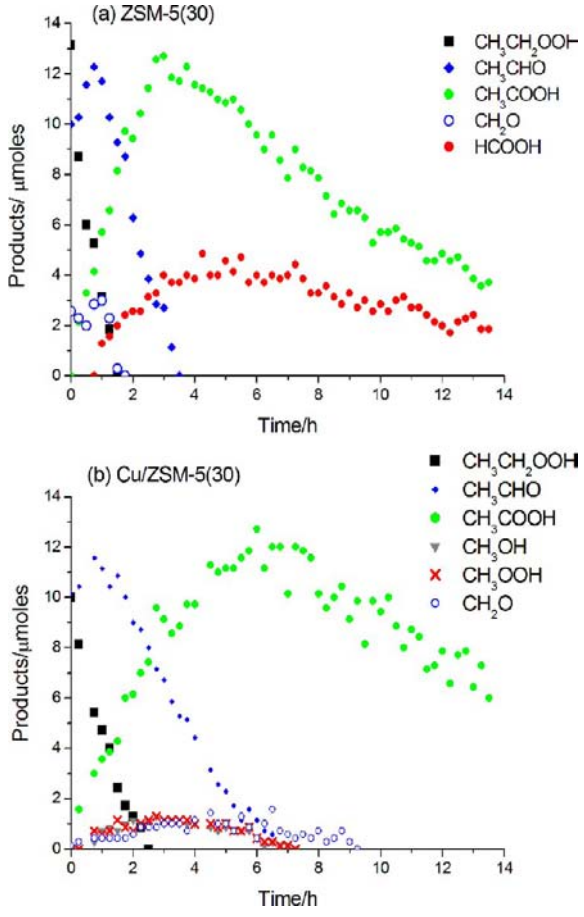

Figure 6. Oxidation of ethyl-hydroperoxide(CH_3CH_2OOH) using (a) ZSM-5(30) and (b) 2.5 wt % Cu/ZSM-5(30) catalysts with H_2O_2 as oxidant studied using time-resolved ^1H NMR experiments.

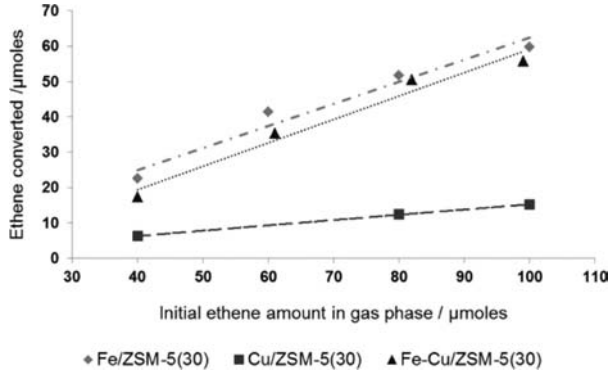

Figure 7. Aqueous phase ethene oxidation over M/ZSM-5(30) catalysts prepared by CVI using H_2O_2 as oxidant. First order plots are obtained in all cases. Test Conditions: 28 mg of catalyst; reaction temperature, 50 °C; time, 0.5 h; stirring rate, 1500 rpm, 0.5 M H_2O_2; 1%C_2H_4/N_2 used for gas feed.

Pd/C catalysts and has been described as an oxidation reaction involving C−C bond cleavage.[8] A C−C bond cleavage reaction should lead to similar levels of aqueous phase oxygenates and gas phase CO_x if the C_1 oxygenates were stable to oxidation in the catalytic system (i.e, the C−OH or C═O(OH) forms CO_x and the CH_3 fragment forms C_1 products). We observed that in the oxidation of both ethanol and acetic acid the selectivity to C_1 products is lower than the selectivity to CO_x using Fe/ZSM-5(30) under the conditions employed (Figures S3, S4 (SI)) indicating the facile oxidation of C_1 oxygenates formed in situ from acetic acid or ethanol to CO_x. This is not the case for the Cu/ZSM-5(30) catalyst for which the levels of C_1 oxygenated and CO_x are similar.

To study the fate of C in ethanol and acetic acid in more detail, we performed the oxidation of ^{13}C labeled ethanol and acetic acid (i.e., $^{12}CH_3{}^{13}CH_2OH$ and $^{13}CH_3{}^{12}C$═O(OH)) with a number of catalysts under modified reaction conditions (i.e., a larger reaction volume to aid the desorption of products, higher substrate concentrations and lower oxidant concentration). The results are summarized in Scheme 1 and Tables S3 and S4 (SI). For both substrates, the level of oxidation followed the trend Fe > Fe−Cu > Cu. Most notably, we observed that both methane and ethane (Table S3 and S4 (SI)) are produced in these stability studies, supporting the hypothesis that C−C cleavage of C_2 reaction products generates methyl radicals, which may subsequently form gas phase alkane products. These methyl radicals, or their termination products (methane and ethane), may also enter the oxidative reaction pathway and produce C_1−C_2 oxygenates. It should also be noted that the C−C bond enthalpy is lower than the C−H bond enthalpy in ethane (377.23 vs 423.29 kJ mol^{-1})[38] and thus the possibility of methyl radicals being derived directly from ethane cannot be ruled out. The presence of methyl radicals in the reaction mixture has also been confirmed using electron paramagnetic resonance trapping experiments (Figure 3). Dimethyl pyrrolidine oxide was used as a water-soluble radical trap under actual reaction

dx.doi.org/10.1021/ja403060n | J. Am. Chem. Soc. 2013, 135, 11087−11099

Scheme 2. Proposed Reaction Network for the Oxidation of Ethane Using H_2O_2 Based on Stability Studies of Reaction Products over ZSM-5(30) Based Catalysts

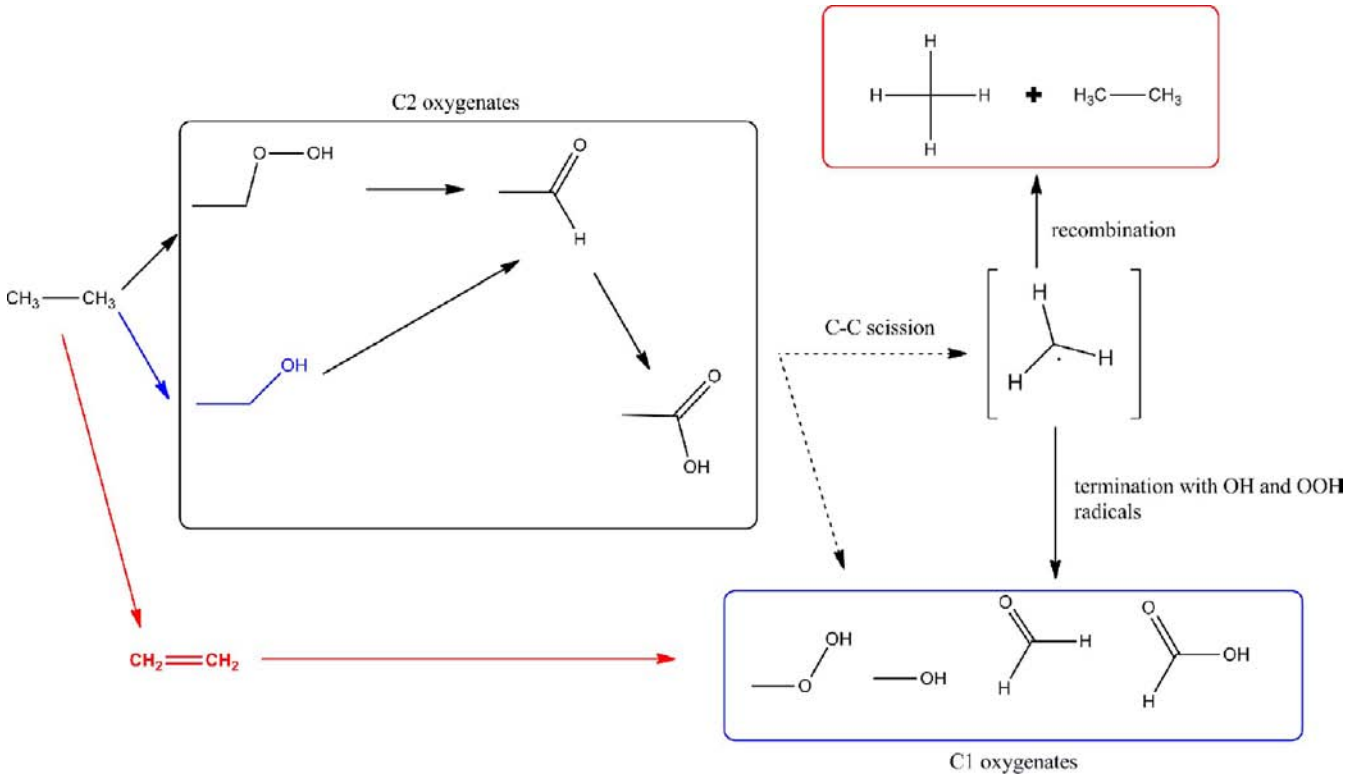

conditions.[20] We observed hydroxyl ($^{\bullet}OH$) and methyl ($^{\bullet}CH_3$) radicals in the reaction mixture, but we cannot exclude the presence of other radical species that may have eluded our analysis due to low concentration or short radical lifetimes.

In the oxidation of $^{12}CH_3{}^{13}CH_2OH$, the Fe and Cu loaded ZSM-5(30) catalysts produce $^{12}CH_3{}^{12}CH_2OH$, indicating a significant contribution from radical recombination reactions. Additionally, the observation of CH_3OOH in the oxidation of both ethanol and acetic acid (Figure S5, Table S3 and S4 (SI)), particularly over the 2.5 wt %Fe/ZSM-5(30) catalyst, further implies that methyl hydroperoxy radicals may be derived from the interaction of methyl radicals and hydroperoxy species or molecular oxygen formed in situ by the decomposition of hydrogen peroxide over the catalysts. Furthermore, the ^1H NMR spectrum of the aqueous phase reaction mixture from the oxidation of $^{13}CH_3{}^{12}C{=}O(OH)$ with Fe/ZSM-5(30) showed two additional peaks corresponding to a ^{12}C product at δ= 4.66 ppm and a ^{13}C product at δ= 4.2 ppm (as evidenced by the splitting pattern due to ^{13}C nuclei). Based on the chemical shift and peak identity (singlet) we tentatively assigned the latter feature to dimethyl tetraoxide or glycolic acid ($^{13}CH_3OO$-$OO^{13}CH_3$ or $^{13}CH_2OH^{12}C{=}O(OH)$ respectively). Dimethyl tetraoxide could be formed by the coupling of two methyl hydroperoxy radicals ($CH_3OO^{\bullet}$) and has been previously studied by ESR methods.[42] Since the presence of alkyl hydroperoxides can be probed by reduction to the corresponding alcohol or aldehyde/ketone,[13] we attempted to investigate the nature of the unknown species using reduction techniques. However, dimethyl tetraoxide has been shown to undergo decomposition to formaldehyde, methanol and molecular oxygen (Russell mechanism, major pathway)[43,44] or to formaldehyde and hydrogen peroxide (Bennett reaction, minor pathway)[44−46] whereas the reduction of glycolic acid would produce acetic acid. In both cases (dimethyl tetraoxide or glycolic acid), the reduction products cannot be easily quantified due to the limitations of our ^1H NMR analysis.

These limitations led us to repeat the oxidation of $^{13}CH_3{}^{12}C{=}O(OH)$ using Fe/ZSM-5(30) but with D_2O as solvent (to reduce the H_2O peak in the ^1H NMR experiment that may obscure product signals) and performing ^1H-NNMR, ^{13}C NMR and Heteronuclear Single Quantum Correlation (HSQC) experiments on a 600 MHz spectrometer (Figure 4 and Figure S5, S6 (SI)). These experiments allowed a greater level of sensitivity than we been able to achieve in previous studies and were facilitated by the ^{13}C label in the substrate. Based on the correlation between the ^1H −NMR signal at δ = 4.18 ppm and ^{13}C NMR signal at δ = 59.35 ppm we assigned the signals to glycolic acid and not dimethyltetraoxide (Figure 3). This product suggest that C−H cleavage in the $-CH_3$ moiety of acetic acid is occurring, probably along with the action of $^{\bullet}OH$ radicals. For the first time we report the ^{13}C shift of CH_3OOH (δ = 64.9 ppm) and also the observation of aqueous $^{13}CO_2$ at δ =124.6 ppm.[47] Additionally, we were able to unambiguously identify $^{13/12}CH_2(OH)_2$ in these experiments based on the ^{13}C shift at δ = 81.7 ppm correlating to ^1H shifts (nearly obscured under the residual water peak).[47] Interestingly we observed a ^1H signal at δ = 5.05 ppm with no observable ^{13}C−H splitting pattern that correlated to a ^{13}C shift at δ = 92 ppm. Based on reference patterns[48,49] and our own studies of authentic samples, we tentatively assign this feature to either hydroxymethyl hydroperoxide or trioxane, both of which are possible in our system and give key mechanistic information about the radical processes involved. We favor the product as hydroxymethyl hydroperoxide since there is no splitting of the ^{13}C signal as would result from ^{13}C labeled trioxane. There

dx.doi.org/10.1021/ja403060n | J. Am. Chem. Soc. 2013, 135, 11087−11099

remains one unknown product that displays a ^{1}H shift at 4.66 ppm and may be correlated to a ^{13}C shift at 73.61 ppm (note the ^{13}C correlation is to the position of the $^{1}H-^{12}C$ signal). This product is, however, only present in our studies on the oxidation of acetic acid and not in the actual reaction solution as evidenced by the reaction spectrum of the oxidation of ethane using Fe/ZSM-5(30) with D_2O as the solvent (Figure S7).

Although our detailed NMR analyses have allowed the identification of all aqueous phase reaction products, the GC-FID technique employed (for gas phase product analysis) did not allow identification of the isotope labels in the gas phase products, but it is highly probable that the CO_x molecules formed in these reactions also contain the ^{13}C label especially as we have detected aqueous phase $^{13}CO_2$ (Figure 4 and Figure S5 (SI)). Furthermore, in the case of $^{13}CH_3{}^{12}C{=}O(OH)$, the $^{13}CH_3$ moiety but not $^{12}C{=}O(OH)$ group was retained in the liquid phase products, suggesting facile oxidation of the carbonyl group to CO_x (Table S4 (SI)). This hypothesis is also supported by similar levels of CO_x to C_1 oxygenates for oxidation of purely ^{12}C ethanol and acetic acid over Cu/ZSM-5(30) and slightly higher levels of CO_x to C_1 oxygenates using Fe/ZSM-5(30) as catalyst (Figures S3 and S4). Hence, one would propose that C_1 oxygenates in the ethane oxidation reaction, if derived solely from C−C bond cleavage reactions involving C_2 oxygenates, would be accompanied by similar levels of CO_x. We note that in the oxidation of ethane a very low level of CO_x (<3%) is observed for all catalysts with significantly higher levels of C_1 oxygenates (>15% for all catalysts except for 2.5 wt % CuZSM-5(30) which still had a higher level of C_1 oxygenates as compared to CO_x, Table 1). The level of oxidation of C_2 to C_1 products in the absence of ethane is much higher than the level of C_1 products observed in ethane oxidation (ca. 40% versus 10−20% for Fe/ZSM-5(30)) under analogous reaction conditions. This may be explained by an enhancement in the stability of the reaction products in the presence of ethane, potentially through competitively adsorbing onto the catalyst active sites, which is in line with our previous observations for methane oxidation. However, considering the disparity between the C_1 to CO_x selectivity, the data indicate that another pathway to C_1 oxygenates may also be in operation, which does not proceed via the cleavage of the C−C bond in ethanol, acetylaldehyde, or acetic acid.

2.3.2. Time-Online Analysis and Oxidation of Ethyl Hydroperoxide. Our observations led us to perform a detailed time-online analysis of the reaction to ascertain if our previously proposed reaction pathway (in methane oxidation) was also in operation with ethane as a substrate, that is, alkane oxidation to the corresponding alcohol via the alkyl hydroperoxide. The time-online analysis for both ZSM-5(30), which contains iron as the catalytically active component, and 2.5 wt %Cu/ZSM-5(30) shows that ethyl hydroperoxide may not be the primary intermediate in this reaction (Figure 5). It is clear from this data that ethyl hydroperoxide is not observed at any significant concentration even after short reaction times, and that the amount of all products generated increases with reaction time in a similar manner. We considered that the catalysts are very active for the oxidation of ethane and thus the absence of ethyl hydroperoxide may be an artifact of the chosen reaction conditions. After altering the reaction conditions over a wide parameter space, we concluded that the reaction profile does not indicate that ethyl hydroperoxide is the primary reaction product, in an analogous manner to methyl hydroperoxide in the methane oxidation reaction (see Figure S8 (SI) as an example).[50] The time-online experiments highlighted that formation of ethyl hydroperoxide does not precede the production of other oxygenates, in particular ethanol, indicating that ethanol may be derived via another mechanistic pathway using these catalysts.

Intrigued by these findings, we then studied the decomposition of ethyl hydroperoxide with our catalysts using ^{1}H NMR experiments in an attempt to monitor which products are derived from this species in the absence of ethane as a reaction component. Ethyl hydroperoxide was first synthesized using a calcined 1.25 wt % Fe/TiO_2 (CVI) catalyst with hydrogen peroxide as the oxidant.[51] A known amount of ethyl hydroperoxide (in D_2O) was subsequently reacted with the catalyst (1.4 mg) and hydrogen peroxide in an NMR tube, and the products analyzed in a time-online experiment at ambient temperature. Both 2.5 wt %Cu/ZSM-5(30) and ZSM-(30) had similar reaction profiles in that ethyl hydroperoxide was sequentially decomposed to acetaldehyde and then acetic acid (Figure 6), while in the absence of the catalyst the substrate was stable to oxidation (Figure S9a (SI)). The 1.25 wt %Fe−1.25 wt %Cu/ZSM-5(30) material was also used as a catalyst in these experiments and displayed the same pattern of reactivity described above (Figure S9b (SI)). The presence of C_1 oxygenates in these experiments stems from the C−C bond scission pathways discussed previously. Our data shows that ethyl hydroperoxide does not decompose to form ethanol over our zeolite-based catalysts, which is in direct contrast to our previous finding that methyl hydroperoxide decomposes to methanol in the methane oxidation reaction when using similar catalyst materials. This finding was further corroborated by performing the ethyl hydroperoxide decomposition reaction in a closed pressurized reactor, such that full analysis of the liquid and gas phase products could be undertaken (Table S5 (SI)). In this experiment there was a good C balance (>90%) and neither CH_4 nor C_2H_4 was observed as gas phase products indicating that two possible decomposition pathways (i) and (ii)[52] are not in operation with our catalysts:

$$CH_3CH_2OOH \rightarrow C_2H_4 + H_2O_2 \quad \text{(i)}$$

$$CH_3CH_2OOH \rightarrow CH_4 + HCOOH \quad \text{(ii)}$$

Since our data is in keeping with previous studies on the decomposition of ethyl hydroperoxide which show that ethyl hydroperoxide decomposes to acetaldehyde,[52−55] we propose that ethanol may be directly produced from the Fe/ZSM-5(30) catalyzed reaction of ethane with hydrogen peroxide. We consider this finding to be pivotal in the design of catalysts, as the controlled decomposition of the alkyl hydroperoxy species to an alcohol would aid in obtaining higher alcohol selectivity in the reaction.

2.3.3. Origin and Role of Ethene in the Reaction. We noted that ethene, an ethane oxidation reaction product, was not observed in our studies for the oxidation of acetic acid, ethanol or the decomposition of ethyl hydroperoxide, leading us to surmise that ethene was being produced directly from ethane. Since it is highly probable that ethene would be oxidized in our system, we carried out the oxidation of ethene such that the initial amount of ethene used as substrate was similar to that observed in the oxidation of ethane. The ethene oxidation rate followed the trend Fe/ZSM-5(30) > Fe−Cu/ZSM-5(30) > Cu/ZSM-5(30), and the major products formed were formic acid, CO_x, and methyl hydroperoxide/methanol, respectively

dx.doi.org/10.1021/ja403060n | J. Am. Chem. Soc. 2013, 135, 11087−11099

(Table 1, entries 13−15). The reaction is first order with respect to ethene (Figure 7), and in all cases significant selectivity to CO_x with low levels of acetic acid was observed. It is clear that if ethene was produced during the reaction, it may be oxidized at varying rates to afford different oxygenates depending on the identity of the metal additive to the ZSM-5 (30) (i.e., Fe, Fe−Cu, or Cu).

To the best of our knowledge, this is the first time that ethene has been reported as a reaction product in the liquid phase oxidation of ethane under mild conditions. Recent computational studies on gas phase ethane oxidation by activated oxygen species, in the form of $[CoO]^+$ and $[Fe{=}O]^+$,[56,57] show that ethanol or ethene can be formed from ethane and this may occur via two mechanistic pathways over the same active site. One pathway encompasses direct H-abstraction from the alkane, followed by radical capture onto the iron-hydroxyl group to produce ethanol. The second pathway, which is based on a fully concerted mechanism using the $[M{=}O]^+$ active site, has multiple routes to the major product, ethene. The abstraction-rebound pathway is similar to our previously proposed mechanism for methane oxidation, although for methane oxidation we favor a concerted mechanism using an iron hydroperoxy species in place of the iron hydroxyl species based on detailed computational studies. The low levels of ethyl hydroperoxide in our reactions (as observed when employing very short reaction times or at low temperature) suggests either the involvement of a M-OOH moiety as we have postulated previously,[20−22] or that it may originate from a process involving ethyl radicals and dissolved molecular oxygen (or hydrogen peroxide). In our system $[Fe{=}O]^+$, as well as other highly reactive oxygen species, can be easily accessed using Fe/ZSM-5(30) and hydrogen peroxide, so we can rationalize the production of ethene based these recent computational findings. Additionally, our experimental data show that Fe−Cu/ZSM-5(30) or Cu/ZSM-5(30) catalysts favor the production of ethene. Since our data also shows that Cu/ZSM-5(30) has a lower ethene oxidation rate as compared to Fe/ZSM-5(30) (Figure 6), we cannot exclude the possibility that the iron sites in ZSM-5(30) initially produce ethene but the Cu species modify the catalyst such that ethene desorbs without further oxidation and is thus detected at higher levels in the gas phase products. However, for Fe−Cu/ZSM-5(30) catalysts, this explanation cannot be applied as ethene is the major reaction product and we demonstrate that the catalyst has an equivalent ethene oxidation rate as Fe/ZSM-5(30) (Figure 6). In the oxidation of ethane, it is clear that Cu is an active component of the catalytic system, in addition to the trace impurities of Fe in the commercial ZSM-5(30) material, as the rate of oxidation of ethane is lower (modified conditions as discussed previously) and the identity/distribution of the reaction products differs greatly for the Cu/ZSM-5(30) catalyst as shown in the time-online plots in Figure 5. At this time, we cannot establish the extent of the contribution of the products of ethene oxidation to the observed catalytic activity due to the complexity of the competing pathways, but taking into account all our findings, we propose the reaction pathway is that outlined in Scheme 2.

3. INITIAL OPTIMIZATION OF THE CATALYTIC ACTIVITY

Finally, we turned our attention to achieving higher conversions of ethane. We studied the effect of hydrogen peroxide concentration and ethane pressure on our most active material,

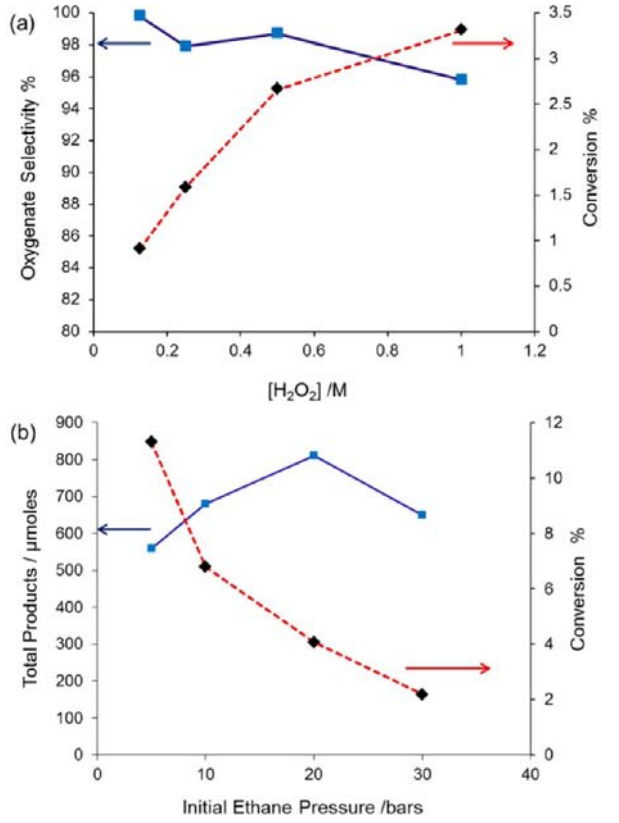

Figure 8. Effect of (a) initial hydrogen peroxide concentration and (b) ethane pressure on the catalytic activity of 1.1 wt % Fe/ZSM-5(30) for ethane oxidation using hydrogen peroxide as oxidant. Test conditions: 28 mg of catalyst; reaction temperature, 50 °C; time, 0.5 h; stirring rate, 1500 rpm, 10 mL reaction volume.

that is, 1.1 wt % Fe/ZSM-5(30) (Figure 8). Increasing the oxidant and substrate concentration has the effect of increasing the catalyst productivity, but we also noted that the conversion was higher at lower ethane pressures because the increase in catalyst productivity is not directly proportional to the increase in the initial amount of ethane present in the system. Thus, we hypothesized that increasing the volume of solvent (to aid dissolution of ethane) along with a lower initial ethane pressure but higher hydrogen peroxide concentration should have a significant effect on the conversion. In this manner, we were able to achieve up to 56% conversion at over 98% selectivity to oxygenated products (ca. 70% to acetic acid) when using 2.5 wt %Fe/ZSM-5(30) as the catalyst (Table 1, entry 16) under these conditions. Using a higher metal loading was necessary in order to improve the conversion at 50 °C, but similar data could be achieved using the 1.1 wt % Fe/ZSM-5(30) catalyst at 70 °C (Figure 9). Under our optimized conditions, the selectivity to ethene was 0.2% selectivity at 56.4% ethane conversion using the 2.5 wt %Fe/ZSM-5(30) catalyst, but the 1.25 wt %Fe-1.25 wt %Cu/ZSM-5(30) catalyst still produced significant amounts of ethene at appreciable conversion of ethane (ca. 13% selectivity at 34% conversion (Table 1, entry 17)). We consider that the high selectivity to ethene and acetic acid with the 1.25 wt %Fe-1.25 wt %Cu/ZSM-5(30) catalyst is similar to the approach of high temperature ODH of ethane in which the simultaneously production ethene and/or acetic acid has been reported,[4] albeit we are using very mild conditions. Although the selectivity to acetic acid is high in our system using Fe based catalysts (generally 50−70%), increasing the acetic acid

dx.doi.org/10.1021/ja403060n | J. Am. Chem. Soc. 2013, 135, 11087−11099

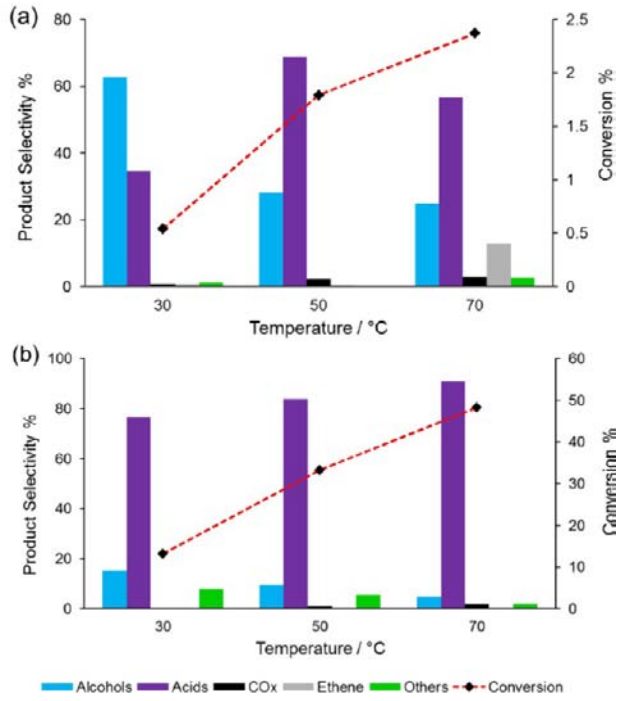

Figure 9. Product distribution as a function of reaction temperature in the oxidation of ethane using hydrogen peroxide and 1.1 wt % Fe/ZSM-5(30) under different test conditions: (a) 28 mg catalyst; H_2O, 0.5 M; reaction volume, 10 mL; C_2H_6, 0.02 mol; stirring rate, 1500 rpm and (b) 54 mg catalyst; H_2O_2, 1 M; reaction volume, 20 mL; C_2H_6, 0.0032 mol; stirring rate, 1500 rpm. "Alcohols" = CH_3OH + CH_3CH_2OH and "Acids" = HCOOH + CH_3COOH.

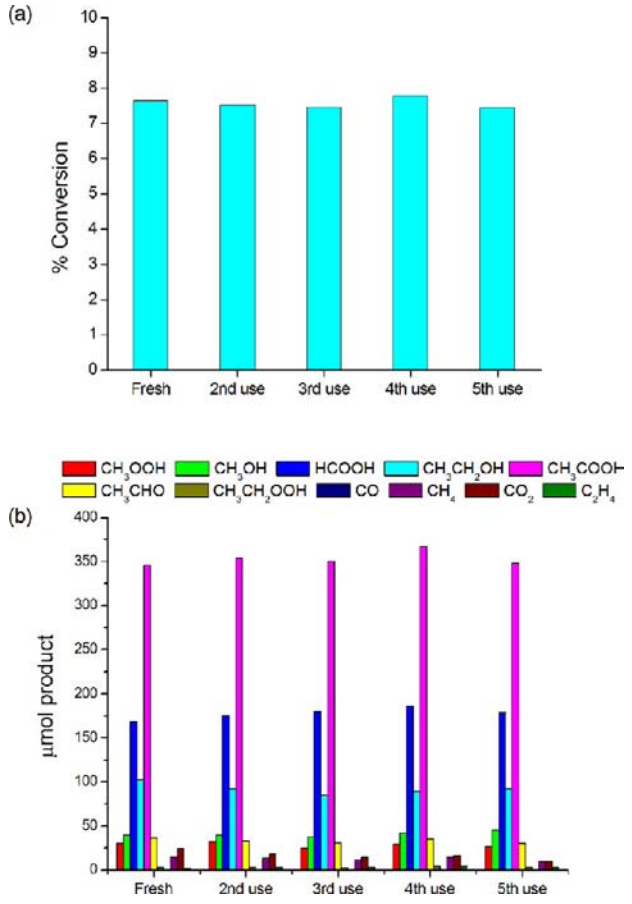

Figure 10. Reuse testing on 1.1 wt % Fe/ZSM-5(30) used in the oxidation of ethane with H_2O_2 as oxidant. (a) Conversion based on carbon and (b) product selectivity based on carbon. Test conditions: 56 mg catalyst; reaction temperature, 50 °C; time, 0.5 h; stirring rate, 1500 rpm, 30 mL reaction volume; $P(C_2H_6)$, 5 bar (40 mL headspace); $[H_2O_2]$, 0.66 M. The catalyst was recovered by filtration under vacuum, washed with water (300 mL), and dried overnight at 120 °C between runs.

selectivity is further hindered by the C−C scission in acetic acid, which tends to produce formic acid, and other competing pathways to C_1 oxygenates. Based on our mechanistic work, we note that the production of ethanol with high selectivity would also be hindered in batch reactor testing since the direct formation of ethanol, its oxidation to acetic acid, and the formation of ethyl hydroperoxide and ethene are all competing pathways. Moreover, it has already been reported that ethanol is only stable at low temperatures over Fe/ZSM-5 materials in the presence of hydrogen peroxide.[58] Our experiments show that ethanol selectivity is indeed highest at low temperature using the 1.1 wt % Fe/ZSM-5(30) catalyst and decreases as conversion increases, even at 30 °C (Figure 9).

We also considered the efficiency of H_2O_2 usage in our catalytic system and found that for H-ZSM-5(30) and the metal loaded derivatives the ratio of H_2O_2 used: products followed the trend H-ZSM-5 > Cu/ZSM-5(30) > Fe−Cu/ZSM-5(30) > Fe/ZSM-5(30) with the iron only catalyst having a usage of 5−6:1. Though the Fe and Fe−Cu catalysts had low decomposition of the oxidant relative to the products we attempted to minimize loss of hydrogen peroxide during the heating stage of the reaction by modifying our protocol so that the reactor was stirred as the temperature was increased to 50 °C over an 11 min period (i.e., the normal time it takes to achieve the 50 °C reaction temperature). This test demonstrated that a stoichometric use of the oxidant was indeed possible in our system (Table S6) along with higher selectivity to the alcohol product, and we will report further optimization using flow reactors in a subsequent publication. Further work with Cu/ZSM-5(30) will also be performed as this material showed the highest selectivity to ethanol in our batch reactions.

Finally, we performed hot filtration tests on the 2.5 wt %Fe and 1.25 wt %Fe-1.25 wt %Cu/ZSM-5(30) catalysts. These tests (Table S7 (SI)) together with recycling testing (Figure 10) showed that the catalysts were reusable under our reaction conditions and that dissolved iron or copper species are not responsible for the observed catalytic activity.

4. CONCLUSIONS

For the first time, we have shown that the Fe/ZSM-5(30) catalyst system is highly selective for the conversion of ethane to a range of oxygenates at appreciable levels of conversion under mild conditions in the aqueous phase. The reaction pathway is more complex than that previously proposed for the methane oxidation reaction using similar zeolite catalysts, and for ethane oxidation a high selectivity to acetic acid with the accompanying formation of formic acid was observed. We have demonstrated that appreciable selectivity to ethene is afforded by both Cu/ZSM-5(30) and Fe−Cu/ZSM-5(30) catalysts. From our studies, it is clear that in order to achieve higher ethanol selectivity with this system, a modification of the catalysts to allow (i) the decomposition of ethyl hydroperoxide to ethanol or (ii) the selective oxidation of ethene (formed in situ from ethane) to ethanol must be found. Hence, our current

dx.doi.org/10.1021/ja403060n | J. Am. Chem. Soc. 2013, 135, 11087−11099

work lays the foundation for future efforts in catalyst design to accomplish this task, but the ability of our system to already produce acetic acid and/or ethene represents an important finding.

■ ASSOCIATED CONTENT

Supporting Information

Spectroscopic data for catalysts, oxidation of ethanol and acetic acid, using zeolite catalysts, studies using ^{13}C-labeled reactants, and reactions using alternative conditions. This material is available free of charge via the Internet at http://pubs.acs.org.

■ AUTHOR INFORMATION

Corresponding Author

Hutch@cardiff.ac.uk

Notes

The authors declare no competing financial interest.

■ ACKNOWLEDGMENTS

This work formed part of the Methane Challenge. The Dow Chemical Company is thanked for their financial support. We thank Dr. Damien Murphy for assistance with the EPR spectroscopy studies.

■ REFERENCES

(1) Alvarez-Galvan, M. C.; Mota, N.; Ojeda, M.; Rojas, S.; Navarro, R. M.; Fierro, J. L. G. *Catal. Today* **2011**, *171*, 15.

(2) Roberts, J. D.; Caserio, M. C. *Basic Principles of Organic Chemistry*; W. A. Benjamin Inc.: Menlo Park CA, 1997.

(3) Rahimi, N.; Karimzadeh, R. *App. Catal., A* **2012**, *398*, 1.

(4) Karim, K.; Al-Hazmi, M. H.; Mamedov, E. In *PCT Int. Appl.*; B01J023-28 ed.; Saudi Basic Ind Corp: 1999.

(5) Chen, N. F.; Ueda, W.; Oshihara, K. *Chem. Commun.* **1999**, 517.

(6) Jones, H. *Platinum Met. Rev.* **2000**, *44*, 94.

(7) Shul'pin, G. B.; Sooknoi, T.; Romakh, V. B.; Suss-Fink, G.; Shul'pina, L. S. *Tetrahedron Lett.* **2006**, *47*, 3071.

(8) Lin, M.; Sen, A. *J. Am. Chem. Soc.* **1992**, *114*, 7308.

(9) Kirillova, M. V.; Silva, J. A. L. d.; Silva, J. J. R. F. d.; Pombeiro, A. J. L. *App. Catal., A* **2007**, *332*, 159.

(10) Lin, M.; Sen, A. *Nature* **1994**, *368*, 613.

(11) Hogan, T.; Sen, A. *J. Am. Chem. Soc.* **1997**, *119*, 2642.

(12) Basickes, N.; Hogan, T.; Sen, A. *J. Am. Chem. Soc.* **1996**, *118*, 13111.

(13) Shul'pin, G. B.; Suss-Fink, G.; Shul'pina, L. S. *J. Mol. Catal. A: Chem.* **2001**, *170*, 17.

(14) Zerella, M.; Mukhopadhyay, S.; Bell, A. T. *Chem. Commun.* **2004**, 1948.

(15) Periana, R. A.; Mironov, O.; Taube, D.; Bhalla, G.; Jones, C. J. *Science* **2003**, *301*, 814.

(16) Otsuka, K.; Hatano, M. *J. Catal.* **1987**, *108*, 252.

(17) Colby, J.; Stirling, D. I.; Dalton, H. *Biochem. J.* **1977**, *165*, 395.

(18) Meinhold, P.; Peters, W. M.; Chen, M. M. W.; Takahashi, K.; Arnold, F. A. *ChemBioChem* **2005**, *6*, 1765.

(19) Xu, F.; Bell, S. G.; Lednik, J.; Insley, A.; Rao, Z.; Wong, L. L. *Angew. Chem., Int. Ed.* **2005**, *44*, 4029.

(20) Hammond, C.; Forde, M. M.; Rahim, M. H. A.; Thetford, A.; He, Q.; Jenkins, R. L.; Dimitratos, N.; Lopez-Sanchez, J. A.; Dummer, N. F.; Murphy, D. M.; Carley, A. F.; Taylor, S. H.; Willock, D. J.; Stangland, E. E.; Kang, J.; Hagen, H.; Kiely, C. J.; Hutchings, G. J. *Angew. Chem., Int. Ed.* **2012**, *51*, 5129.

(21) Hammond, C.; Jenkins, R. L.; Dimitratos, N.; Lopez-Sanchez, J. A.; Ab Rahim, M. H.; Forde, M. M.; Thetford, A.; Murphy, D. M.; Hagen, H.; Stangland, E. E.; Moulijn, J. M.; Taylor, S. H.; Willock, D. J.; Hutchings, G. J. *Chem.—Eur. J.* **2012**, *18*, 15735.

(22) Hammond, C.; Dimitratos, N.; Jenkins, R. L.; Lopez-Sanchez, J. A.; Kondrat, S. A.; Ab Rahim, M. H.; Forde, M. M.; Thetford, A.; Taylor, S. H.; Hagen, H.; Stangland, E. E.; Kang, J.; Moulijn, J. M.; Willock, D. J.; Hutchings, G. J *ACS Catal.* **2013**, *3*, 689.

(23) Ovanesyan, N. S.; Shteinman, A. A.; Dubkov, K. A.; Sobolev, V. I.; Panov, G. I. *Kinet.* **1998**, *39*, 792.

(24) Xia, H. A.; Sun, K. Q.; Sun, K. J.; Feng, Z. C.; Li, W. X.; Li, C. *J. Phys. Chem. C* **2008**, *112*, 9001.

(25) Smeets, P. J.; Woertink, J. S.; Sels, B. F.; Solomon, E. I.; Schoonheydt, R. A. *Inorg. Chem.* **2010**, *49*, 3573.

(26) Perez-Ramirez, J.; Groen, J. C.; Bruckner, A.; Kumar, M. S.; Bentrup, U.; Debbagh, M. N.; Villaescusa, L. A. *J. Catal.* **2005**, *232*, 318.

(27) Kumar, A. S.; Perez-Ramirez, J.; Debbagh, M. N.; Smarsly, B.; Bentrup, U.; Bruckner, A. *Appl. Catal., B* **2006**, *62*, 244.

(28) Perez-Ramirez, J.; Kumar, M. S.; Bruckner, A. *J. Catal.* **2004**, *223*, 13.

(29) Hensen, E. J. M.; Zhu, Q.; Janssen, R. A. J.; Magusin, P.; Kooyman, P. J.; van Santen, R. A. *J. Catal.* **2005**, *233*, 123.

(30) Jacobs, P. A.; Von Ballmoos, R. *J. Phys. Chem.* **1982**, *86*, 3050.

(31) Bordiga, S.; Platero, E. E.; Arean, C. O.; Lamberti, C.; Zecchina, A. *J. Catal.* **1992**, *137*, 179.

(32) Kustov, L. M.; Kazansky, V. B.; Beran, S.; Kubelkova, L.; Jiru, P. *J. Phys. Chem.* **1987**, *91*, 5247.

(33) Quin, G.; Zheng, L.; Xie, Y.; Wu, C. *J. Catal.* **1985**, *95*, 609.

(34) Schuetze, F. W.; Roessner, F.; Meusinger, J.; Papp, H. *Stud. Surf. Sci. Catal.* **1997**, *112*, 127.

(35) Morrow, B. A. *Stud. Surf. Sci. Catal.* **1990**, *57*, A161.

(36) Hellmut, G. K. Characterisation by IR spectroscopy In *Verified Synthesis of Zeolitic Materials*, 2nd ed.; Robson, H., Ed.; Elsevier: Amsterdam, 2001; p 69.

(37) Lide, D. R. *CRC Handbook of Chemistry and Physics*, 88th ed.; CRC Press: Boca Raton, FL, 2005.

(38) Blanksby, S. J.; Ellison, G. B. *Acc. Chem. Res.* **2003**, *36*, 255.

(39) Actual metal loading as determeined by ICP analysis is given in the Supporting Information. The experimental metal loading of CVI catalysts is slightly less than the theoretical amount.

(40) Under similar conditions to the work with sMMO(low pressure, 12 min reaction time) by Colby et al., the productivity of our system is 95.2 mol (products) kg (cat)$^{-1}$ h^{-1} .

(41) Forde, M. M; Grazia, B. C; Armstrong, R.; Jenkins, R. L.; Ab Rahim, M. H.; Carley, A. F.; Dimitratos, N.; Lopez-Sanchez, J. A.; Taylor, S. H.; Mc Keown, N. B.; Hutchings, G. J. *J. Catal.* **2012**, *290*, 177.

(42) Schuchmann, P. H.; Sonntag, C. V. *Z. Naturforsch., B* **1984**, *39B*, 217.

(43) Russell, G. A. *J. Am. Chem. Soc.* **1957**, *79*, 3871.

(44) Cooper, W. J.; Cramer, C. J.; Martin, N. H.; Mezyk, S. P.; O'Shea, K. E.; Sonntag, C. v. *Chem. Rev* **2009**, *109*, 1302.

(45) Bennett, J. E.; Summers, R. *Can. J. Chem.* **1974**, *52*, 1377.

(46) Bennett, J. E. *J. Chem. Soc., Faraday Trans.* **1990**, *86*, 3247.

(47) Morooka, S.; Wakai, C.; Matubayasi, N.; Nakahara, M. *J. Phys. Chem. A* **2005**, *109*, 6610.

(48) Gab, S.; Hellpointner, E.; Turner, W. V.; Korte, F. *Nature* **1985**, *316*, 535.

(49) Xamena, F. X. L. i.; Arean, C. O.; Spera, S.; Merlo, E.; Zecchnia, A. *Catal. Lett.* **2004**, *95*, 51.

(50) Reactions with lower oxidant level (0.25 M), lower catalyst mass (10−14 mg) or performed at lower temparature (30 °C) showed that in short reaction times (1−5min) ethanol and ethyl hydroperoxide were formed in similar amounts with the other major reaction products being acetylaldehyde and acetic acid over both ZSM-5(30) and Cu/ZMS-5(30).

(51) 1.25 wt % Fe/TiO_2(CVI) produces 0.003 M ethyl hydroperoxide in D_2O when the reaction is performed at 30 °C for 20 h. Acetylaldehdye is the other major product.

(52) Chen, D.; Jin, H.; Wang, Z.; Zhang, L.; Qi, F. *J. Phys. Chem. A* **2011**, *115*, 602.

(53) Hou, H.; Li, J.; Song, X.; Wang, B. *J. Phys. Chem. A* **2005**, *109*, 11206.

(54) Ignatyev, I. S.; Xie, Y.; Allen, W. D.; S., H. F., III. *J. Chem. Phys.* **1997**, *107*, 141.
(55) Harris, E. J. *Proc. R. Soc. London, Ser. A* **1939**, *173*, 126.
(56) Zhao, L.; Lu, X.; Li, Y.; Chen, J.; Guo, W. *J. Phys. Chem. A* **2012**, *116*, 3282.
(57) Sun, X. I.; Huang, X. R.; Li, J.; Huo, R. P.; Sun, C. C. *J. Phys. Chem. A* **2012**, *116*, 1475.
(58) Kuznetsova, E. V.; Savinov, E. N.; Vostrikova, L. A.; Parmon, V. N. *Appl. Catal., B* **2004**, *51*, 165.